EXPERIMENTAL INVESTIGATIONS ON TRIBOLOGICAL ASSESSMENT AND NO$_x$ EMISSIONS OF PALM BIODIESEL BLENDED WITH OLEIC ACID AND ETHANOL

KARTHIC RAJA M[1]; KAMALESH A SORATE[1]* and PURNANAND V BHALE[1]

ABSTRACT

Tribological behaviour of biodiesel should be investigated to get confidence for long-term engine usage. Also, the higher nitrous oxide (NO$_x$) level from the biodiesel-fueled engine is observed. Tribological assessment and engine performance of lower blends of palm biodiesel (B10, B20) are available in the literature. Due to limited reserves of fossil fuels, the demand for biodiesel is increasing day by day. To fulfil this demand, the higher blends of biodiesel (such as B80, B90) should be investigated. Hence, this study aimed to investigate the tribological and NO$_x$ assessment of the higher blends of palm biodiesel. Palm biodiesel was produced by transesterification and blended with oleic acid (OA) and ethanol (E). Biodiesel blends such as 100% biodiesel (B100), 80% biodiesel + 20% oleic acid (B80OA20), 90% (80% biodiesel + 20% oleic acid) + 10% ethanol (B80OA20E10), 90% biodiesel+10% oleic acid (B90OA10), and 95% (90% biodiesel + 10% oleic acid) + 5% ethanol (B90OA10E5) were prepared. Pin on disc machine was used for tribological study and diesel engine was used for NO$_x$ analysis. Nearly 40% reduction in wear and 48% reduction in friction were observed for B80OA20 compared to B90OA10, while B90OA10E5 exhibited the lowest frictional force among all the test fuels. During tribological assessment, two blends B80OA20 and B80OA20E10 showed satisfactory performance and were further studied for NO$_x$ analysis. Also, these two blends lower NO$_x$ emissions by 12% and 2%, respectively, compared to B100.

INTRODUCTION

Fatty acid methyl ester, commonly known as biodiesel, is derived from edible, nonedible feedstocks and waste cooking oils, recently microalgae (Atmanli, 2020). Biodiesel can be produced by conventional transesterification, hydrodynamic cavitation reactor, electrolysis, ultrasonication, and microwave methods (Tabatabaei *et al.*, 2019). The thermophysical properties of biodiesel were found to be comparable with petro-diesel (Verma *et al.*, 2021). Biodiesel showed an increase in fuel consumption and a decrease in brake thermal efficiency. In addition, biodiesel showed less exhaust emissions except nitrous oxide (NO$_x$) compared to diesel (Tamilselvan *et al.*, 2017).

Unlike other feedstocks used for biodiesel production, oil palm is a perennial crop, thereby being a reliable raw material source. Palm oil in crude and refined form accounts for over one-third of vegetable oil production. Palm oil cultivation stood at nearly 73 million tonnes for 2018-2019, estimated to rise to 240 million tonnes by 2050 (Tillis, 2019). The palm oil yield per hectare of a plantation is over ten times higher than other feedstocks (Mekhilef *et al.*, 2011). Palm oil can be transesterified into biodiesel using a 12:1 methanol to oil molar ratio, NaOH as catalyst

[1] Renewable and Sustainable Energy Laboratory,
Department of Mechanical Engineering,
Sardar Vallabhbhai National Institute of Technology,
Surat, Gujarat, India.

* Corresponding author's email: kasorate@med.svnit.ac.in

(0.6 w/v), and a reaction temperature of 60°C for 60 min (Benjumea *et al.*, 2008). In other study, palm biodiesel was prepared using a transesterification process (reaction temperature 60°C for 60 min; 10:1 methanol to oil molar ratio, KOH as catalyst (1.4 w%; stirring 250 rpm). Engine performance of B20 blend showed that brake specific fuel consumption (BSFC) increases while brake thermal efficiency (BTE) and emission decreases except NO_x as compared to diesel (Rosha *et al.*, 2019). *Table 1* shows the European Standards of NO_x emission.

The lubrication properties of fuel/biofuel can increase the engine's life. Biodiesel generally possess better lubricity than diesel (Mishra and Goswami, 2018). Tribological properties depend upon the load and temperature. Diesel engine components such as fuel pumps and injectors are lubricated by fuel itself. The wear and friction properties of the biodiesel samples should be equivalent to or better than that of the conventional diesel used in automobiles. It was found that the addition of nanoparticles and alcohol improves the lubricity of B30 (diesel-palm-sesame) biodiesel (Mujtaba *et al.*, 2021). For Aamla biodiesel, the tribological properties were affected at higher loads and higher temperatures compared to low loads and lower temperatures (Singh *et al.*, 2018). The lubricating characteristics of biodiesel in terms of friction and wear decrease as the temperature of the fuel rises (Haseeb *et al.*, 2010). Compared to diesel, the wear and friction coefficients of B20 (palm and cottonseed biodiesel) were lower.

The long hydrocarbon chains of biodiesel decreased the friction and improved lubrication (Jamshaid *et al.*, 2022). Biodiesel was found corrosive to engine components when stored for long durations (Sorate and Bhale, 2013, 2018), but its better lubricity resulted in less friction and wear (Fazal *et al.*, 2014). The wear and friction coefficient reduces as the biodiesel concentration increases from B10 to B100. It's because of the compositional nature of biodiesel (Fazal *et al.*, 2013). Tertiary blends of biodiesel improved the lubrication property of palm (B10) biodiesel when blended with plastic pyrolysis biodiesel and waste cooking oil biodiesel (Awang *et al.*, 2022). Through tribological testing, biolubricants were found the most promising lubricant. Jatropha biolubricant was tested for tribological characteristics. The use of a 20% Jatropha biolubricant blend was found to be efficient in minimising friction and wear on the pins used in the tests (Anand *et al.*, 2022)

Engine performance of palm oil biodiesel blends was found to be satisfactory except NO_x emissions (Lim and Teong, 2010). Palm oil biodiesel contains about 49.2% oleic acid, palmitic acid (43.3%), and stearic acid (5.4%). Oleic acid is a good carrier of hydrogen and oxygen (Ali *et al.*, 2016). Hydrogen concentration (up to 5%) demonstrates a minor reduction in NO_x. However, as H_2 concentration rises, NO_x levels rise as well. A controlled increase in oleic acid content resulted in a reduction in NO_x emissions for Karanja (Pongamia) biodiesel (Dinesha *et al.*, 2018; Mohan *et al.*, 2021). The use of B10, B20 biodiesel from rice bran and Pongamia, along with hydrogen enrichment (7 L/min), can improve brake thermal efficiency by up to 6%. However, when compared to diesel, the NO_x from blended biodiesel with hydrogen increases by up to 13% (Kanth and Debbarma, 2021). Diesel, on the other hand, produced more NO_x than algae, or Jatropha oil (Krishania *et al.*, 2020). Water emulsified biodiesel can reduce harmful emissions. Emulsified palm biodiesel (B10, B15 and B20) were prepared using ultrasonication. A decrease in NO_x was observed for emulsified fuel. However, the calorific value decreases, and viscosity increases with an increase in the blending ratio (Azahari *et al.*, 2016).

The properties of biodiesel can be improved by adding additives. Further improvements to the combustion phenomenon can be made, resulting in lower emissions (Gaur *et al.*, 2022). The addition of 2% ethanol lowers the smoke emissions. It was found that adding ethanol to canola biodiesel reduces emissions (Öztürk and Can, 2022). Compared to diesel, biodiesel emits more NO_x due to oxygen in biodiesel. NO_x emissions were revealed as a result of a higher combustion temperature. There have also been initiatives taken across the globe on the production of second-generation ethanol. The plant-based feedstock would help to improve the farmer's income. Although ethanol is not an ideal alternative fuel for diesel engines, it can be added to reduce fuel viscosity, and density as well as improve the cold flow performance (Yilmaz *et al.*, 2018).

The binary blends of waste oil biodiesel with higher alcohols (propanol, n-butanol, and 1-pentanol) on semi-low temperature combustion in diesel engines showed lower NO_x emissions (Atmanli and Yilmaz, 2020). On the other hand, the ternary blends of diesel, crude vegetable oil and n-butanol showed an increase in oxides of nitrogen (Atmanli *et al.*, 2015). Combustion of diesel, rapeseed oil, and n-butanol in turbocharged engines showed an increase in NO_x formation (Ileri *et al.*, 2016a; Örs

TABLE 1. NO_x EMISSION STANDARDS OF EUROPEAN HEAVY DUTY DIESEL ENGINE

Tier	Euro I	Euro II	Euro III	Euro IV	Euro V	Euro VI
Year	1992	1996	2000	2005	2008	2013
NO_x level (g/kWh)	8.0	7.0	5.0	3.5	2.0	0.4

et al., 2020). Moreover, a quaternary blend of diesel, waste oil biodiesel, soybean oil and higher alcohols showed an 11.9% reduction in oxides of nitrogen (Yilmaz *et al.*, 2018). The optimised diesel, butanol, and cottonseed oil blend also showed decreased NO$_x$ for variable speed engines (Atmanli *et al.*, 2016). Along with experimental methods, predicting methods such as the response surface method and least-squares support vector machine models can be used for engine performance and emission parameters (Ileri *et al.*, 2016b).

The web of science data analysis was done on 10th October, 2023 for the availability of research papers in the area of biodiesel, palm biodiesel, NO$_x$ reduction and tribology. A total 44 849 research articles were found. Out of this, 4273 articles were found related to palm biodiesel. Out of 4273, only 140 were found on NO$_x$ reduction and 46 were found on tribology. The data is presented as shown in *Figure 1*.

Sufficient work related to tribological behaviour and emissions of lower blends such as B10, and B20 of biodiesel with conventional diesel has been reported in the literature. The novelty of this research paper is that higher blends (B80 and B90) of palm biodiesel on tribology and emission are investigated which is very exiguous in the open literature. Also, studies related to the reduction of NO$_x$ emission by means of blending with oxygenated compounds are very limited. Therefore, the main aim of this study is to investigate experimentally the tribological assessment and NO$_x$ emissions of higher blends of palm biodiesel blended with oleic acid and ethanol. The materials and methodology related to biodiesel feedstock selection, production, characterisation, tribological characteristics, engine testing, and results are discussed in subsequent sections. The flowchart of the work performed is shown in *Figure 2*.

MATERIALS AND METHODS

Refined palm oil was obtained from the nearby convenience store, while diesel was purchased from a local fuel station. A local supplier provided methanol, KOH (potassium hydroxide), OA (oleic acid), and ethanol.
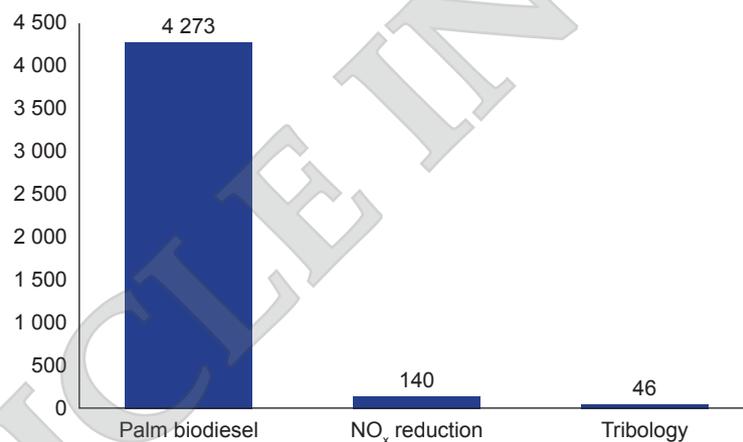

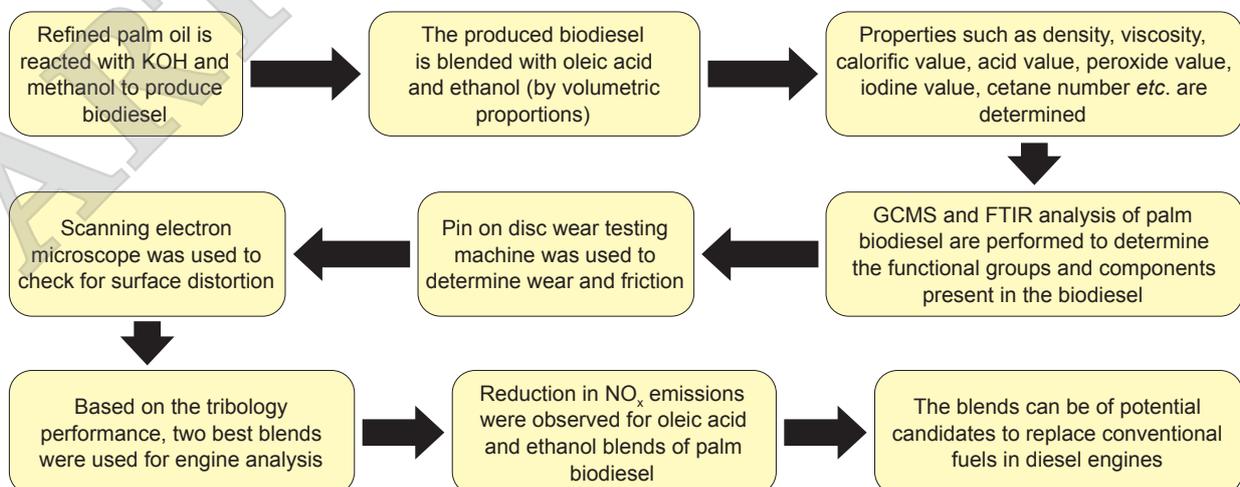*Figure 1. Number of research articles available in the area of palm biodiesel.*

Figure 2. Flowchart of the work.

Transesterification

The palm oil was mixed and heated to 60°C using a magnetic stirrer. A borosilicate condenser with water as a coolant was used to cool the methanol solution. Methanol - oil molar ratio of 1:7 and 1.2% w/v of KOH were used as the catalyst. The stirring speed was maintained at 700 rpm. The reaction was carried out for an hour while maintaining the temperature at 60°C. The resulting solution was placed in a decantation flask and left undisturbed for an hour. The crude glycerol and the biodiesel separated due to the density difference. Glycerol was removed, and the remaining solution was water-washed to remove dissolved KOH and other impurities. The fatty acid methyl ester was heated in the oven to vaporise moisture in the solution. The entire process of transesterification is depicted in *Figure 3*.

The blending of the test fuels was carried out based on volumetric proportions, and five test fuels, namely B100 (100% palm biodiesel), B90OA10 (90% palm biodiesel + 10% Oleic Acid), B90OA10E5 [95% (90% palm biodiesel + 10% oleic acid) + 5% ethanol], B80OA20 (80% palm biodiesel + 20% oleic acid), and B80OA20E10 [90% (80% palm biodiesel + 20% oleic acid) + 10% ethanol], were prepared.

Characterisation

The quality of the produced biodiesel depends on many factors, such as the properties of feedstock, the catalyst used, reaction parameters, *etc.* Certain physio-chemical parameters must be evaluated to check the quality of produced biodiesel. Some of the critical attributes of liquid fuel include density, kinematic viscosity, calorific value, pour point, cloud point, acid value (AV), peroxide value (PV), iodine number, saponification number, and cetane number (CN). All biodiesel and its blends were characterised to ensure compliance with ASTM (American Society for Testing and Materials) and EN (European Standards) standards.

The energy content of the biodiesel blends was determined using a LECO 350 bomb calorimeter. The density was measured as per ASTM D1298 standard. The viscosity of the test fuels was assessed using a Redwood viscometer. The flashpoint was measured with Cleveland open-cup apparatus. A cloudy white appearance was observed at the temperature known as cloud point. The pour point is the temperature where biodiesel loses its flowability and is determined by adding 3°C to the observed temperature. The detailed procedure for determining the AV, PV, and CN is mentioned in Annexures A, B and C respectively. FTIR (Fourier Transform InfraRed) spectroscopy is the most widely used tool to predict the functional groups present in biodiesel. FTIR spectroscopy was carried out using a Shimadzu IRAffinity-1S spectrometer. The procedure of FTIR is mentioned in Annexure D. The instruments used for evaluating the characteristics of the test fuels of the study are shown in *Figure 4*.

The contents of the fatty acids in palm biodiesel were determined using gas chromatography and mass spectrometry (SHIMATZU QP 2010). By comparing their retention durations to those of a typical methyl ester of fatty acids, the composition of methyl ester was determined.

Configuration of Pin on Disc (POD) Wear Tester

Ducom POD wear tester was used to perform a tribological assessment of the sample. Pins made of stainless steel were used in the process. This test measured the amount of wear and frictional force. The apparatus consists of a pin that provides a normal load. A uniform volume flow of 10 mL/min of test fuel was maintained over the disc to ensure proper contact with the pin. The rpm, load, time, and offset distance from the centre are given as input to the wear and friction monitor. Diesel was used to compare with the results of biodiesel and its blends. Scanning Electron Microscope (SEM) was used to study the surface of pin tips post POD testing. The experimental setup and the specifications of the tribometer are described in *Figure 5* and *Table 3* respectively.
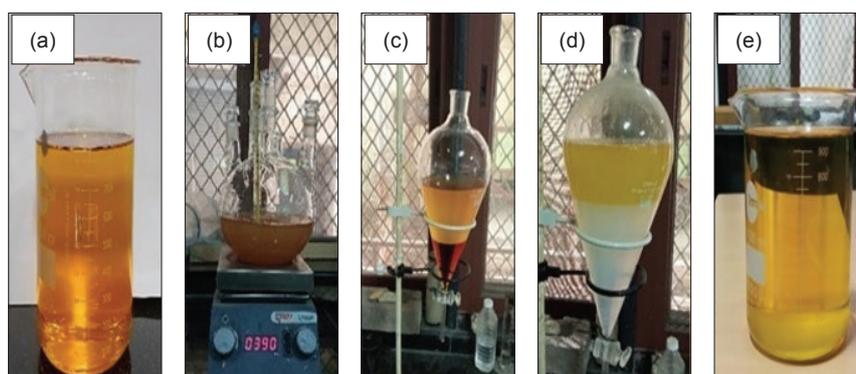

Figure 3. Transesterification process (a) refined palm oil, (b) reactor vessel, (c) glycerol separation, (d) water washing, and (e) palm biodiesel.

Figure 4. Instruments used for the characterisation study.

Figure 5. Experimental setup of the POD wear tester and SEM used in the study.

TABLE 3. SPECIFICATIONS OF POD WEAR TESTER AND PARAMETERS SET FOR THE STUDY

Make	Ducom
Disc speed	200-2000 rpm
Normal load range	5-200 N
Wear range	± 2 mm
Least count	1 ± 1 % µ
Frictional force range	0 to 200 N
Accuracy	0.1 ± 2.0% N
Load	5 kg
Rotating speed	200 rpm
Sliding distance	1500 m
Time	720 s
Temperature	30°C

Configuration of Engine Test Rig

Based on the characterisation and tribological study, conventional diesel and three biodiesel test fuels B100, B80OA20 and B80OA20E10, were chosen for engine testing. A computerised test rig consisting of four-strokes, a 5.2 kW diesel engine,

and Testo gas analyser was used to evaluate engine performance, emissions, and combustion of test fuels. The specifications and details of instrumentation used in the engine setup and the experimental setup of the test rig are depicted in *Table 4* and *Figure 6* respectively.

Figure 6. Experimental setup of the engine test rig.

TABLE 4. SPECIFICATIONS OF THE CI ENGINE

Make	Kirloskar TV1
General details	Four-strokes, CI, vertical, constant speed, water-cooled, single cylinder
Bore × stroke (mm)	87.5 × 110
Compression ratio	17.5
Capacity (cc)	661
Rated output (kW)	5.2 at 1500 rpm
Piezo sensor make	PCB Piezotronics, Model HSM111A22
Inlet valve opening / Inlet valve closing	4.5º before TDC / 35.5º after BDC
Exhaust valve opening / Exhaust valve closing	35.5º before BDC / 4.5º after TDC
Injection advance	23º before TDC

Note: CI - Compression ignition; BDC - Bottom dead centre; TDC - Top dead centre.

The load to the engine was applied with a dynamometer. The constituents of exhaust gases were measured using an emission analyser. Data on fuel flow, torque, water flow rate, and other parameters were obtained using a data-gathering system.

Uncertainty Analysis

The validity of the obtained results depends upon the instruments' accuracy and techniques used in the process. The characterisation, engine testing, and tribological studies involve the use of many instruments and equipment, which leads to the need to perform uncertainty analysis. Each experiment was carried out thrice, and the average was presented. The uncertainties of the individual experiments carried out in this research work are shown in *Table 5*. The uncertainty of the results was calculated using the root mean square approach and was found to be ± 2.1%.

$$\text{Overall uncertainty} = \sqrt{\begin{array}{c} CV^2 + Density^2 + KV^2 + AV^2 + \\ PV^2 + Wear^2 + Friction^2 + BTE^2 + \\ BSFC^2 + CO^2 + NO_x^2 + CO_2^2 \end{array}}$$

$$= \sqrt{\begin{array}{c} 0.5^2 + 0.4^2 + 0.6^2 + 0.5^2 + 0.6^2 + \\ 0.2^2 + 0.7^2 + 0.7^2 + 0.4^2 + 0.6^2 + \\ 0.3^2 + 1.2^2 \end{array}}$$

$$= \pm 2.1\%$$

where, KV is kinematic viscosity, AV is acid value, PV is peroxide value, BTE is brake thermal efficiency, BSFC is brake specific fuel consumption, CO is carbon monoxide and CO_2 is carbon dioxide.

RESULTS AND DISCUSSION

The results obtained from the experimentation of biodiesel and its blends are discussed in the following section. The characterisation, tribology, and engine testing of the blended test fuels will also be discussed in this section.

Characterisation of Biodiesel Blends

The characterisation of biodiesel and blends was carried out, and is listed in *Table 6*. Blending OA with B100 reduced the CV and PV but increased the density and acid value. The blending of OA increased the acid value beyond the permissible limit. The viscosity of the OA was also higher than pure biodiesel. 10% blending restricts the kinematic viscosity within the allowable limit. Further blending takes it beyond the permissible limit of 6 mm²/s as per ASTM standards. The cold flow properties of OA measured is lower than B100. Thus, blending reduced the cloud and pour point, and ethanol addition further augmented them. The addition of ethanol reduced the calorific value of the blended test fuels.

The FTIR analysis of the palm biodiesel produced by transesterification is illustrated in *Figure 7*. The bending vibration at a wavenumber of 1743.65 cm⁻¹ and 1168.862 cm⁻¹ represents the C=O and C-O bonds of the esters, respectively. The stretching band at 2854.648 cm⁻¹ denotes the formation of alkanes. These peaks reflect the ester component in the biodiesel sample (Abdullah *et al.*, 2017). A significant difference was seen in the fingerprint region corresponding to 900-1500 cm⁻¹. The rocking vibration of C-H can be noted at 721.37 cm⁻¹. A more substantial peak was observed for the biodiesel sample than palm oil, indicating the conversion of triglycerides to fatty acid methyl esters during transesterification (Kamaronzaman *et al.*, 2020). The comparison plot indicates fatty acid methyl ester formation obtained post-transesterification.

From GC-MS analysis, the percentages of palmitic acid (C16:0), oleic acid (C18:1), linoleic acid (C18:2) and stearic acid (C18:0) in palm biodiesel are respectively 41.25, 38.91, 11.65 and 5.73.

TABLE 5. UNCERTAINTY ANALYSIS OF EXPERIMENTATION

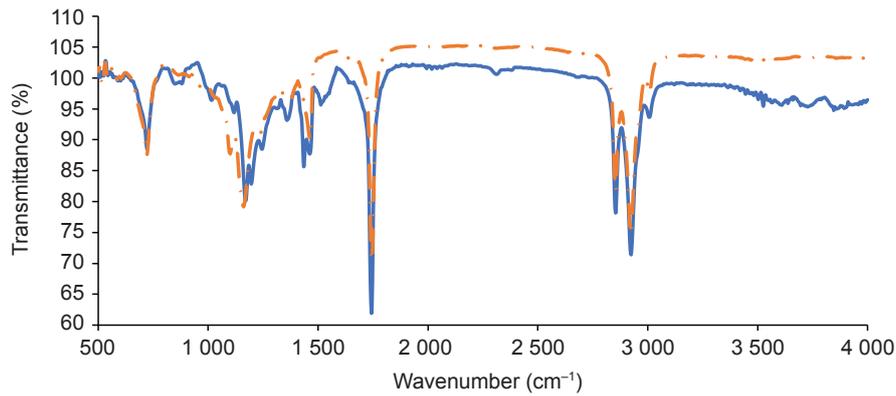| No	Instrument used	Accuracy	Uncertainty (in %)
1	Calorific value (CV)	± 0.5%	± 0.5
2	Density	± 0.01 g/cc	± 0.4
3	Kinematic viscosity (KV)	± 1.0%	± 0.6
4	Acid value (AV)	± 0.1 mL	± 0.5
5	Peroxide value (PV)	± 0.2 mL	± 0.6
5	Wear	± 1.0% µm	± 0.2
6	Friction	± 2.0% N	± 0.7
7	BTE	± 0.5%	± 0.7
8	BSFC	± 0.5 kg/kWh	± 0.4
9	CO_2	± 0.2% vol	± 0.6
10	NO_x	± 10 ppm	± 0.3
11	CO	± 10 ppm	± 1.2

Figure 7. FTIR spectroscopy of palm oil and B100.

TABLE 6. MEASURED PHYSIO-CHEMICAL CHARACTERISTICS OF BIODIESEL AND ITS BLENDS

Property	Standards	Limit	B100	B90OA10	B90OA10E5	B80OA20	B80OA20E10	OA	Diesel
Calorific value (kJ/kg)	ASTM D6751	-	40493.17	40014.52	39013.07	39827.91	38845.12	39516.20	42000
Cloud point (°C)	ASTM D2500	-3 to -12	17	11	8	5	3	1	-6
Pour point (°C)	ASTM D97	-15 to -16	14	8	5	2	0	-2	-30
Kinematic viscosity @ 40°C (cSt)	ASTM D445	1.9 to 6.0	4.59	5.65	5.1646	8.16	5.7732	18.74	4.6
Density (kg/m³)	ASTM D1298	820-860	866.67	873	869	881	876	906.67	830
Flashpoint (°C)	ASTM D93	130	176	182	85	185	92	192	58
Acid value (mg KOH/g)	ASTM D664	0.5 maximum	0.369	17.403	16.3158	34.465	30.44025	198.5	-
Free fatty acid (%)			0.185	8.74	8.1988	17.32	15.296	99.75	-
Peroxide value (meq/kg)	AOAC 965.33	-	16.614	13.745	14.730	10.896	13.698	2.904	-
Iodine value (gI$_2$/100 g)	EN-14111	-	57.975	61.17	58.111	64.364	57.927	89.921	-
Saponification value	-	-	207.452	206.53	196.206	205.65	185.05	198.25	-
Cetane number	-	47 minimum	59.565	58.968	54.463	58.3717	51.067	53.5985	48

Pin on Disc (POD) Wear Testing

The following section discusses the friction characteristics, wear analysis, and surface morphology of the pins used in POD testing.

Friction analysis. Lubrication is required to reduce the friction in different engine components, thereby reducing wear and improving the engine's life span. The frictional force obtained for each sample with respect to sliding distance is as shown in *Figure 8a*. The fluctuation is due to the variation in surface roughness and contact area of the pin tip with the disc. The blends and additives of palm biodiesel show a lesser frictional force than that of conventional diesel. A significant reduction in friction force was observed upon ethanol addition. The B80OA20E10 reduced the frictional force by 43% on average with reference to B80OA20, thereby showing the least frictional force compared to all the test fuels. The presence of ester groups (RCOOR) provides sufficient adhesion to form a tribofilm with the pin surface, exhibiting better anti-friction capability (Chan *et al.*, 2018). The higher viscosity of sample oil reduces the metal-to-metal contact during the experimentation (Kurre and Yadav, 2023). This explains the reduction in friction force on addition upon blending of OA to B100. The addition of ethanol further reduced the frictional force of the blend. The high polarity of ethanol aids in reducing the contact between pin and the disc (Sorate and Bhale, 2015).

Wear analysis. Figure 8b demonstrates the wear in the pins with respect to distance. The amount of wear generated in each pin tip of different test fuels was calculated by finding the difference in wear at the start and end of the experimentation. The wear was the highest in the B100 sample, with 53.03 µm after the entire run. Nearly 25% reduction in wear has been recorded for B90OA10 compared to B100. The wear observed in the pins by B80OA20 was lower than diesel. The addition of

OA has significantly reduced the wear of the pin. Nearly 40% reduction in wear and 48% reduction in friction was observed for B80OA20 compared to B90OA10. The B90OA10E5 reduced wear by 11% compared to B90OA10. On the contrary, 10% ethanol additive to B80OA20 increases the wear by 70% to 40.47 µm. The blending of OA by 20% has reduced the wear by nearly 55% compared to B100 sample. The reduction in wear of B80OA20 and B90OA10 might be due to the higher composition of unsaturated compounds than B100, which aids in forming a stronger layer of film between the metals (Zaid *et al.*, 2021). The shorter carbon chains in the esters and higher polarity of compounds enhance the lubricity of the test sample (Sorate and Bhale, 2015). Hence, ethanol having higher polarity, act as an emulsifier forming strong emulsions with B80OA20.

Surface morphology analysis. The surface morphology of the pin post-wear testing for the test fuels is shown in *Figure 9*. The obtained micrographs can be correlated with the friction force and wear, as shown in *Figure 8a* and *8b*. Indentations are present for B100 in the direction parallel to the wear, indicating abrasion. The B100 has a lower viscosity than OA blends, leading to higher surface contact with the disc. The images for the diesel show severe delamination of the pin surface (Maleque *et al.*, 2000). Surface distortion in the form of pits can be observed in B90OA10 and B80OA20 samples. Bubbles in the order of 300 µm² can be observed for the B80OA20E10 sample. This may be due to the agglomeration of ethanol molecules on the pin surface. The level of micro-pitting was observed to be higher for B90OA10 compared with the B80OA20 sample.
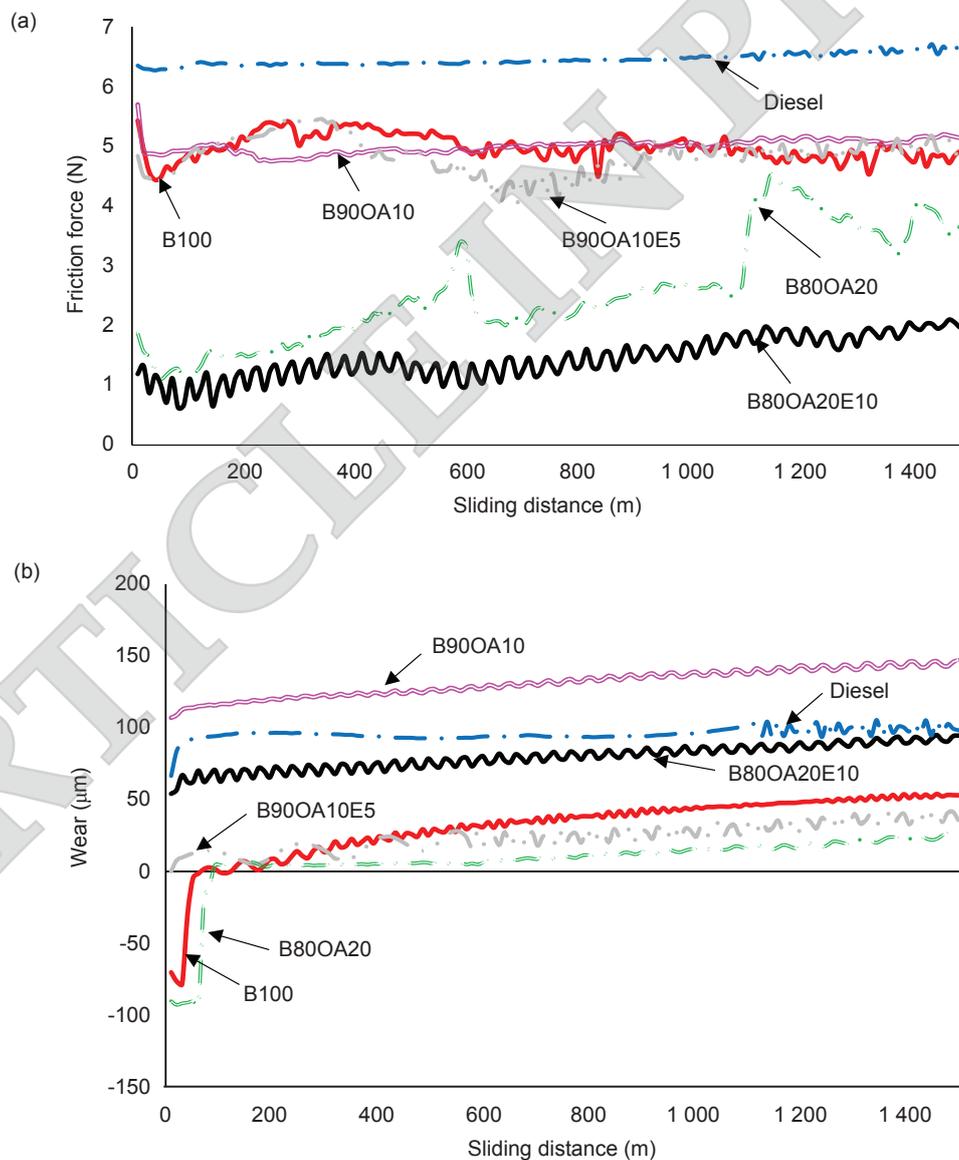

Figure 8. (a) Friction force variation of different test fuels with respect to sliding distance, and (b) wear of pins for different test fuels with respect to sliding distance.
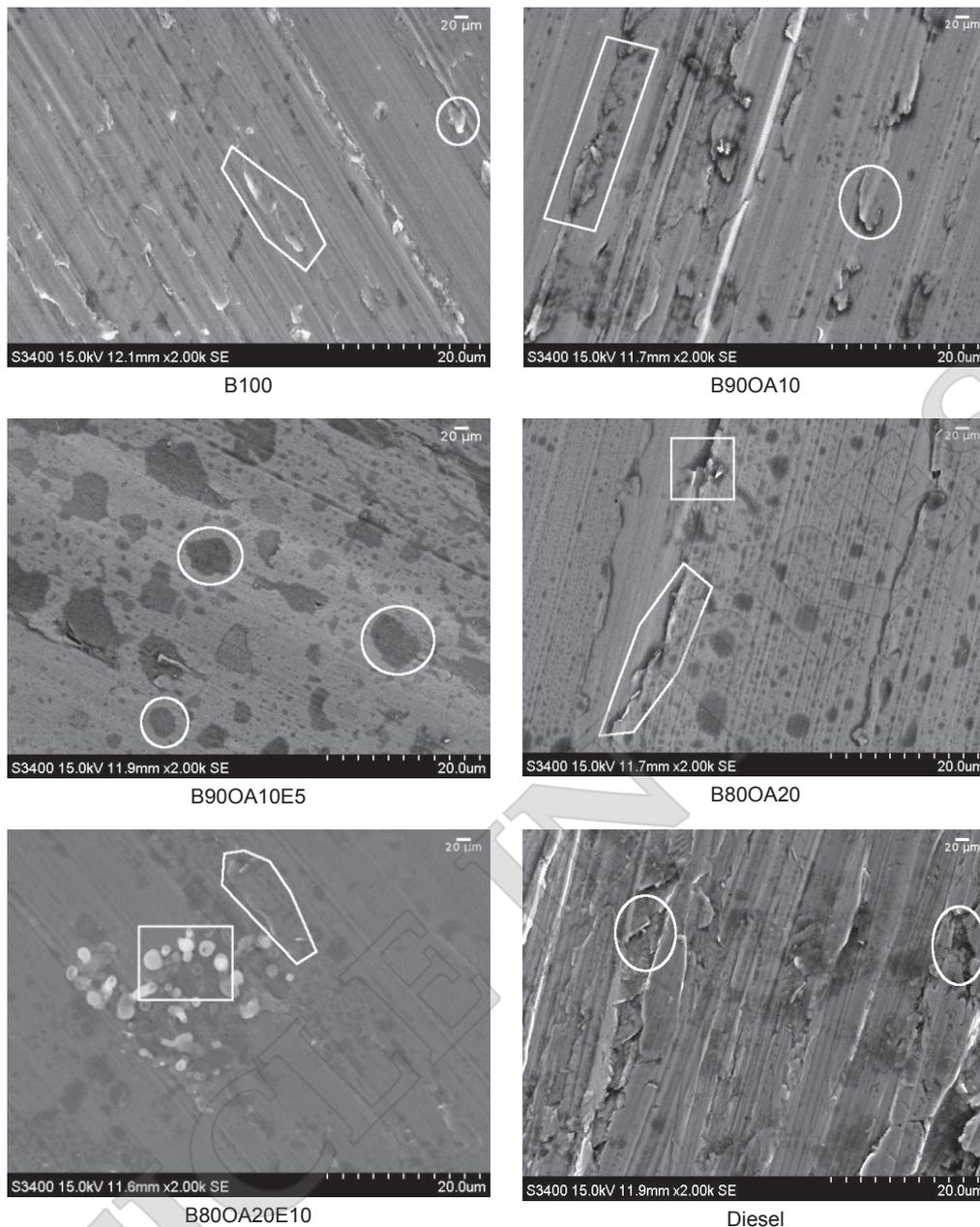
Figure 9. SEM micrographs of pin tip after POD wear test.

Engine Performance, Combustion and Emission Analysis

This section discusses the engine performance, combustion, and emission of B100, B80OA20, B80OA20E10 and diesel.

Brake thermal efficiency (BTE). BTE is the ratio of brake power available at the output of the shaft to the heat supplied by the fuel. *Figure 10a* presents the BTE of all the test fuels varying with brake mean effective pressure (BMEP). Conventional diesel exhibits the highest BTE of 35.22%, followed by B80OA20, B100, and B80OA20E10 of 33.49%, 32.29% and 32.02%, respectively, at BMEP of 5.5 bar.

Performance is improved using fuel with a higher heating value and lower flash point. Complete fuel combustion is ensured by high cylinder pressure and temperature, leading to greater efficiency. The result obtained for the conventional diesel was consistent with the literature (Rajamohan *et al.*, 2022). The higher density and kinematic viscosity of biodiesel blends account for the decrease in BTE compared to diesel (Sakthivel *et al.*, 2018). On the contrary, adding OA to B100 has shown a positive effect on BTE, increasing it by 3% compared with B100. This can be explained by the fact that OA contains oxygenated molecules, which improve fuel burning (Mohan *et al.*, 2021). The lower calorific value of B80OA20E10 has led to lower BTE among

all the samples. Due to ethanol's lower boiling point, the fuel mixture burns ineffectively during combustion (Rahiman *et al.*, 2022).

Brake specific fuel consumption (BSFC) (kWh). The fuel consumption for a unit kilowatt hour of power generation for different test fuels is shown in *Figure 10b*. The brake power is directly proportional to BMEP; hence, fuel consumption decreases with a rise in BMEP. Conventional diesel shows the lowest BSFC of 0.23 kg/kWh at 5.5 bar BMEP while B100 and B80OA20E10 exhibit BSFC of 0.28 kg/kWh. The BSFC increases by 0.01 kg/kWh to 0.28 kg/kWh on addition of 10% ethanol to B80OA20. Increased calorific value and reduced viscosity of the diesel help in the finer mixing of the fuel, reducing fuel consumption (Rajamohan *et al.*, 2022). A very minuscular effect in fuel consumption is observed between B100 and B80OA20, with the latter showing a slightly higher consumption than the former. The increase in BTE of B80OA20 compared to B100 has led to a reduction in BSFC.

Peak pressure. Peak cylinder pressure for various fuels with respect to crank angle (in °) is shown in *Figure 11a*. The 0° indicates the TDC of the engine cylinder. A slight ignition delay can be observed

for all the test fuels due to the atomisation and premixing stage of combustion. However, the B100 sample attained peak pressure at 47.51 bar at 8° compared to B80OA20 at 9°. The B80OA20 exhibits nearly a 15% rise in the peak pressure to 55.43 bar compared to the 47.95 bar attained by the B100 sample. Higher viscosity and density of B80OA20 cause poor fuel atomisation. Thus, fuel gets accumulated, and a greater quantity of fuel gets injected inside the combustion chamber, leading to a rise in the peak pressure. *Table 6* illustrates that B80OA20 possesses a viscosity nearly double that of B100. Ethanol addition to B80OA20 has lowered the blend's viscosity and CN. However, it has raised the peak pressure to 60.87 bar, comparable to 61.99 bar attained by conventional diesel. This may be due to the vaporisation of ethanol before the ignition phase (Rahiman *et al.*, 2022). The lower CN and higher latent heat of vaporisation of B80OA20E10 would have augmented the peak pressure (Kim *et al.*, 2020). The peak pressure relies on the oxidation level attained during the premixing phase of combustion.

Cumulative heat release rate (CHRR). CHRR was plotted with respect to the crank angle (in °), as shown in *Figure 11b*. The rate at which the flame consumes the unburned mass of fuel charge is
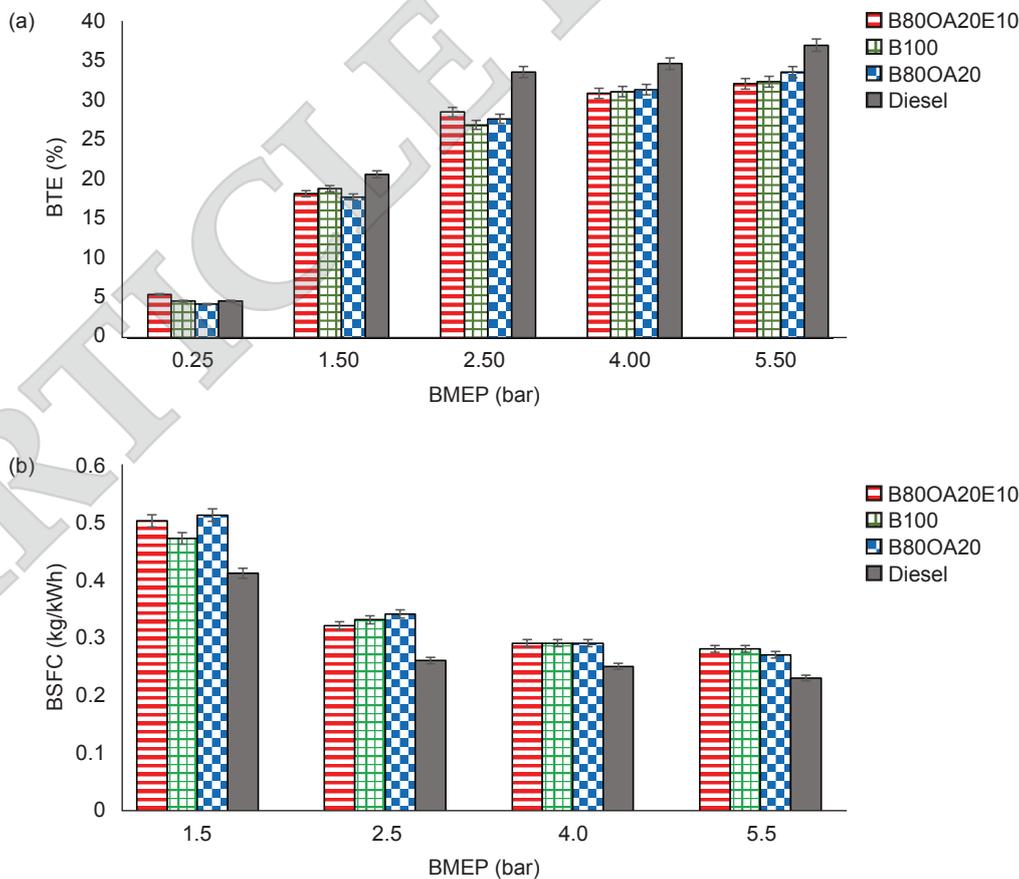

Figure 10. (a) Variation in BTE with respect to BMEP, and (b) variation in BSFC with respect to BMEP.

known as CHRR. The diesel exhibits the highest CHRR of 1.08 kJ at 63°, while the B100 shows the least CHRR of 0.61 kJ at 47°. Lower CN has increased the ignition delay of diesel compared to biodiesel and its blends. The shorter ignition delay period caused by the higher CN of B100 allows fuel to ignite more quickly and easily. The higher CN of B100 has lowered the ignition delay period compared to B80OA20 and B80OA20E10. Adding OA increased the CHRR by 36% to 0.83 kJ at 53°, and B80OA20E10 recorded a CHRR of 0.95 kJ at 57°. The increase in CHRR was due to the increase in adiabatic flame temperature (Kim *et al.,* 2020). The higher oxygenated and hydrogen components in the B80OA20 than in B100 aid in complete combustion, resulting in higher CHRR (Mohan *et al.,* 2021). The higher viscosity and density lead to fuel accumulation in the cylinder, increasing the fuel available for combustion (Santhoshkumar *et al.,* 2019).

Exhaust gas temperature. The exhaust gas temperature of different test fuels is shown in *Figure 12a*. Diesel showed the highest temperature of 321°C, followed by B100 and B80OA20E10 at 320°C and 314°C at 5.5 bar. All the test fuels show an increase in temperature with BMEP. B80OA20 has a greater viscosity, resulting in poor atomisation. The lower calorific value of biodiesel and higher CN leads to lower exhaust gas temperature (Enweremadu and Rutto, 2010). Higher temperature augments the formation of NO$_x$ emissions (Rajamohan *et al.,* 2022).

NO$_x$ emissions. As shown in *Figure 12b*, an increasing trend in NO$_x$ emissions with the BMEP can be observed for all test fuels. Higher in-cylinder temperature and pressure favor NO$_x$ emissions. NO$_x$ majorly consists of NO and NO$_2$. NO formation is profound at lean air-fuel ratio. At lean fuel conditions, combustion NO is formed.
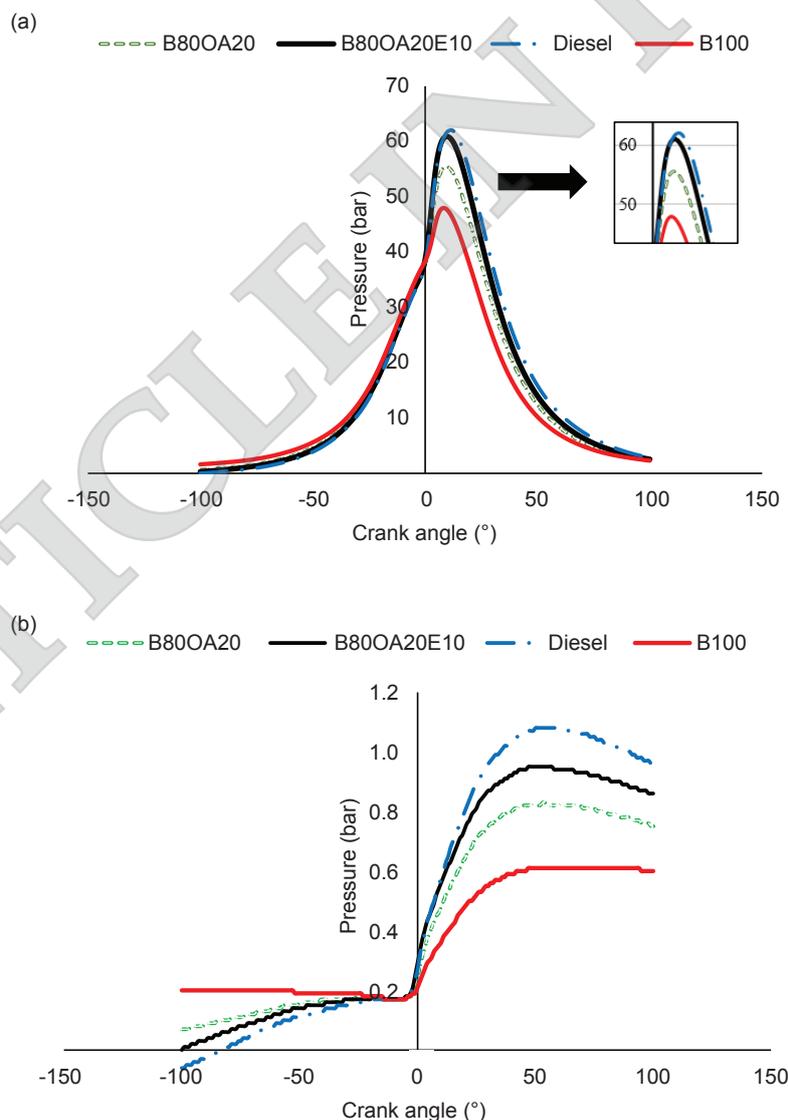

Figure 11. (a) Peak pressure with respect to crank angle, and (b) cumulative heat release rate (CHRR) with respect to crank angle.

Zeldovich mechanism governs the NO_x formation (Shote *et al.*, 2019). At lean fuel conditions, more air is available for combustion. As a result, the nitrogen and oxygen present in the air starts reacting with the fuel at a higher temperature, increasing NO_x emissions. Adding OA has shown a positive impact in reducing NO_x emissions. B100 has shown the highest NO_x emission of 769 ppm among all the samples at 5.5 bar BMEP. The oxygen in the fatty acids of biodiesel aids atmospheric nitrogen's reaction, thereby augmenting NO_x formation. However, with the addition of 20% OA by volume, the emissions have decreased by 17.3% to 636 ppm. OA has a higher viscosity, lower boiling point, and higher evaporation rate; hence it supports NO_x emission reduction when blended with biodiesel. The higher density of palm biodiesel gives a higher residence time for the fuel to stay in the high-temperature region, which increased the NO_x emission. Another reason might be due to the higher bulk modulus of compressibility of biodiesel, advancing the injection timing. The presence of hydrogen concentrations also helps in reducing NO_x emissions, and OA ($C_{18}H_{34}O_2$), being a carrier of hydrogen, aids in the reduction of NO_x. Oxygenated compounds reduce the flame temperature and thus improve combustion efficiency. NO_x emissions increased by 11.3% for B80OA20E10. Adding ethanol reduced the blend's density and viscosity, resulting in lower NO_x emission than B100. Similar trends were also observed by some researchers (Lee *et al.*, 2021).

CO emissions. Figure 12c displays the change in CO emissions with BMEP for all test fuels. A decreasing trend is noticed for all the test fuels. Adding ethanol by 10% to B80OA20 increased the emissions by nearly 25% to 571 ppm at 5.5 bar

pressure. While performing the combustion in a stoichiometric air-fuel ratio, the hydrocarbons present in the fuel would get oxidised to CO_2 and H_2O (Lee *et al.*, 2021). In fuel-rich conditions, these hydrocarbons do not oxidise to CO_2 and instead form CO, indicating an incomplete oxidation condition. A lower carbon to hydrogen ratio in B100 might have reduced CO emissions (Muhammed Niyas and Shaija, 2022). The addition of ethanol leads to viscosity reduction and enhances the atomisation of fuel in the injector. However, the results indicate a higher CO emission for B80OA20E10. Ethanol's higher latent heat and evaporative cooling effect would have resulted in partial combustion. Additionally, higher ignition delay would have increased the CO emissions (Shahir *et al.*, 2015).

CO_2 emissions. Figure 12d indicates CO_2 emissions, and all the test fuels show an increasing trend with BMEP. The B80OA20E10 shows the highest emission of 7.560% volume, followed by 7.400% volume from the B100 sample and 7.353% volume by diesel at 5.5 bar BMEP. The B80OA20 sample showed the lowest emission of 7.230% volume. The CO_2 emissions get augmented with the rise in BMEP for all the test fuels. The complete oxidation of the fuel leads to the formation of CO_2 (Rajamohan *et al.*, 2022). The higher CO_2 emissions indicate the degree of complete combustion. The formation of CO_2 is highly favourable for renewable sources of fuel as it aids in maintaining a closed carbon cycle, thereby reducing global warming (Sakthivel *et al.*, 2019). An explicit trade-off is observed in the sample's CO and CO_2 emissions trends for B100, B80OA20, and diesel. However, B80OA20E10 showed the highest CO and CO_2 emissions. A higher quantity of oxides of carbon is produced when oxygen is available in fuel.
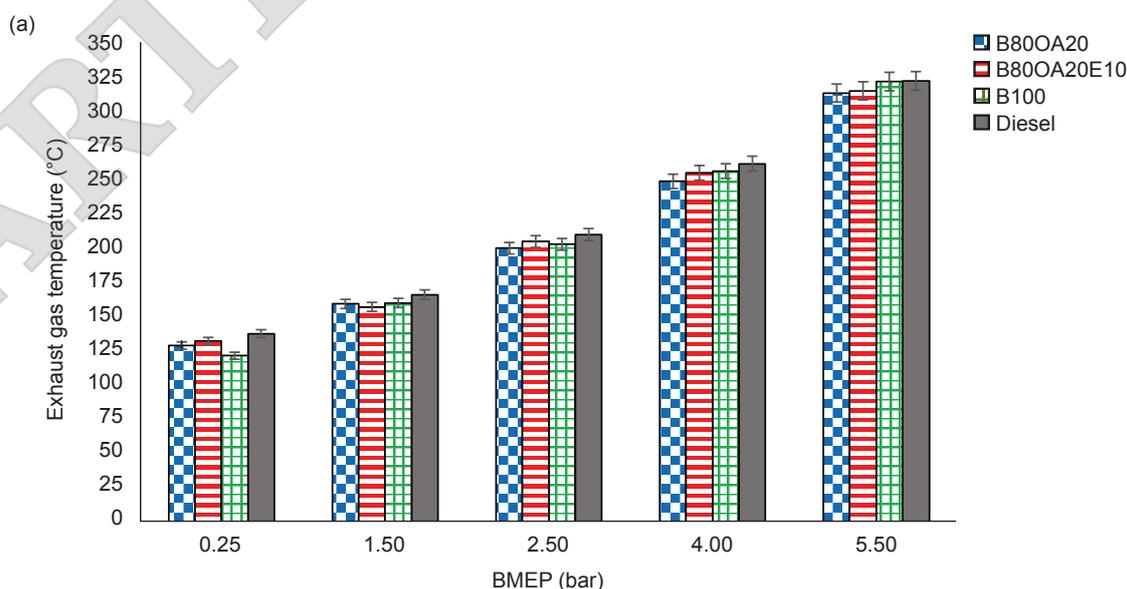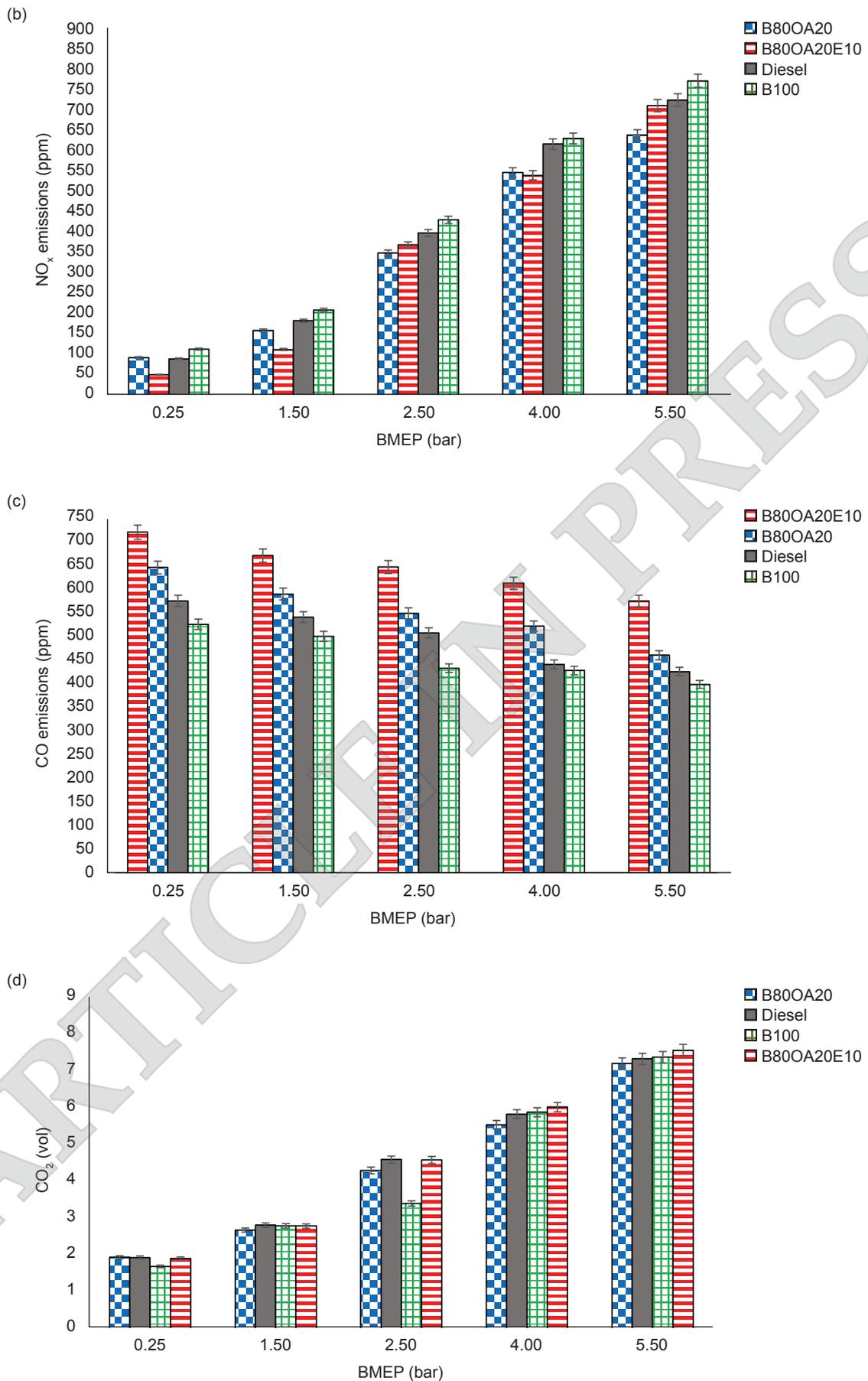
Figure 12. (a) Exhaust gas temperature with respect to BMEP, (b) NO$_x$ emissions with respect to BMEP, (c) CO emissions with respect to BMEP, and (d) CO$_2$ emissions with respect to BMEP.

CONCLUSIONS

The prepared biodiesel and blends were characterised by following the required standards. The properties of prepared biodiesel and blends were found to be comparable with diesel. A tribological assessment was carried out using POD machine. A decrease in frictional force for biodiesel and its blends was observed. Wear and SEM analysis showed comparable results of biodiesel and its blends with diesel. The following conclusions are 1) Analysis of friction force, wear and SEM images showed that B80OA20 and B80OA20E10 blends showed better results than B90OA10 and B90OA10E5. Wear reduced by 48% in B80OA20 when compared with B90OA10, while B80OA20E10 showed the least frictional force. 2) The blends namely, B80OA20 and B80OA20E10 were studied for engine and emission analysis and compared with diesel and B100. However, the tested blend showed less BTE in comparison with diesel but the addition of OA with palm biodiesel (B80OA20) showed a 3% increase in BTE when compared to B100. On the other hand, adding ethanol in B80OA20 showed minuscular decrease in BTE compared to B100. An increase in cylinder pressure is observed in B80OA20 and B80OA20E10 compared to B100. 3) The critical contribution of this study is that B80OA20 and B80OA20E10 showed a decrease in NO_x level and improved tribological behaviour when compared to B100 and diesel. Also, these two blends lower NO_x emissions by 12% and 2%, respectively, compared to B100 and 4) Hence, the higher blends of palm biodiesel with oleic acid were practical from tribological and NO_x emission points of view.

The authors recommend future studies on the engine material compatibility, oxidation stability, and long-term endurance of palm biodiesel blended with oleic acid (B80OA20) and ethanol (B80OA20E10) that will help to gain more confidence amongst engine manufacturers and the automotive industry.

ACKNOWLEDGEMENT

REFERENCES

Abdullah; Rahmawati Sianipar, R N; Ariyani, D and Nata, I F (2017). Conversion of palm oil sludge to biodiesel using alum and KOH as catalysts. *Sustain. Environ. Res., 27(6)*: 291-295.

Ali, O M; Mamat, R; Abdullah, N R and Abdullah, A A (2016). Analysis of blended fuel properties and engine performance with palm biodiesel-diesel blended fuel. *Renew. Energy*, *86*: 59-67.

Anand, G; Yick, J and Kabir, S N (2022). Rheological and tribological properties of *Jatropha curcas* biolubricants at various blend concentrations. *Biofuels*, *13(5)*: 623-630.

Atmanli, A (2020). Experimental comparison of biodiesel production performance of two different microalgae. *Fuel*, *278*: 118311.

Atmanli, A and Yilmaz, N (2020). An experimental assessment on semi-low temperature combustion using waste oil biodiesel/C3-C5 alcohol blends in a diesel engine. *Fuel*, *260*: 116357.

Atmanli, A; Ileri, E; Yuksel, B and Yilmaz, N (2015). Extensive analyses of diesel-vegetable oil-n-butanol ternary blends in a diesel engine. *Appl. Energy*, *145*: 155-162.

Atmanli, A; Ileri, E and Yilmaz, N (2016). Optimization of diesel-butanol-vegetable oil blend ratios based on engine operating parameters. *Energy*, *96*: 569-580.

Awang, M S N; Mohd Zulkifli, N W; Zulkifli, S; Kalam, M A; Mohd Yusoff, M N A; Daud, W; Ahmad, M H and Abbas, M M (2022). Effect of diesel-palm biodiesel fuel with plastic pyrolysis oil and waste cooking biodiesel on tribological characteristics of lubricating oil. *AEJ - Alex. Eng. J., 61(9)*: 7221-7231.

Azahari, S R; Salahuddin, B B; Noh, N A M; Nizah, R and Rashid, S A (2016). Physico-chemical and emission characterization of emulsified biodiesel/diesel blends. *Biofuels*, *7(4)*: 337-343.

Benjumea, P; Agudelo, J and Agudelo, A (2008). Basic properties of palm oil biodiesel-diesel blends. *Fuel*, *87(10)*: 2069-2075.

Chan, C-H; Tang, S W; Mohd, N K; Lim, W H; Yeong, S K and Idris, Z (2018). Tribological behaviour of biolubricant base stocks and additives. *Renew. Sustain. Energy Rev.*, *93*: 145-157.

Dinesha, P; Jagannath, K and Mohanan, P (2018). Effect of varying 9-octadecenoic acid (oleic fatty acid) content in biofuel on the performance and emission of a compression ignition engine at varying compression ratio. *Biofuels*, *9(4)*: 441-448.

Enweremadu, C C and Rutto, H L (2010). Combustion, emission and engine performance characteristics of used cooking oil biodiesel - A review. *Renew. Sustain. Energy Rev.*, *14(9)*: 2863-2873.

Fazal, M A; Haseeb, A S M A and Masjuki, H H (2013). Investigation of friction and wear characteristics of palm biodiesel. *Energy Convers. Manag.*, *67*: 251-256.

Fazal, M A; Haseeb, A S M A and Masjuki, H H (2014). A critical review on the tribological compatibility of automotive materials in palm biodiesel. *Energy Convers. Manag.*, *79*: 180-186.

Gaur, A; Dwivedi, G; Baredar, P and Jain, S (2022). Influence of blending additives in biodiesel on physiochemical properties, engine performance, and emission characteristics. *Fuel*, *321*: 124072.

Haseeb, A S M A; Sia, S Y; Fazal, M A and Masjuki, H H (2010). Effect of temperature on tribological properties of palm biodiesel. *Energy*, *35(3)*: 1460-1464.

Ileri, E; Atmanli, A and Yilmaz, N (2016a). Comparative analyses of n-butanol-rapeseed oil-diesel blend with biodiesel, diesel and biodiesel-diesel fuels in a turbocharged direct injection diesel engine. *J. Energy Inst.*, *89(4)*: 586-593.

Ileri, E; Atmanli, A; Yilmaz, N; Karaoglan, A; Okkan, U and Kocak, M S (2016b). Predicting the engine performance and exhaust emissions of a diesel engine fuelled with hazelnut oil methyl ester: The performance comparison of RSM and LSSVM. *J. Energy Resour. Technol.*, *138(5)*: 052206.

Jamshaid, M; Masjuki, H H; Kalam, M A; Zulkifli, N W M; Arslan, A and Qureshi, A A (2022). Experimental investigation of performance, emissions and tribological characteristics of B20 blend from cottonseed and palm oil biodiesels. *Energy*, *239*: 121894.

Kamaronzaman, M F F; Kahar, H; Hassan, N; Hanafi, M F and Sapawe, N (2020). Analysis of biodiesel product derived from waste cooking oil using Fourier transform infrared spectroscopy. *Mater. Today Proc.*, *31*: 329-332.

Kanth, S and Debbarma, S (2021). Comparative performance analysis of diesel engine fuelled with hydrogen enriched edible and non-edible biodiesel. *Int. J. Hydrog. Energy*, *46(17)*: 10478-10493.

Kim, H Y; Ge, J C and Choi, N J (2020). Effects of ethanol-diesel on the combustion and emissions

from a diesel engine at a low idle speed. *Appl. Sci.*, *10(12)*: 4153.

Krishania, N; Rajak, U; Nath Verma, T; Kumar Birru, A and Pugazhendhi, A (2020). Effect of microalgae, tyre pyrolysis oil and *Jatropha* biodiesel enriched with diesel fuel on performance and emission characteristics of CI engine. *Fuel*, *278*: 118252.

Kurre, S K and Yadav, J (2023). A review on bio-based feedstock, synthesis, and chemical modification to enhance tribological properties of biolubricants. *Ind. Crops Prod.*, *193*: 116122.

Lee, C C; Tran, M-V; Tan, B T; Scribano, G and Chong, C T (2021). A comprehensive review on the effects of additives on fundamental combustion characteristics and pollutant formation of biodiesel and ethanol. *Fuel*, *288*: 119749.

Lim, S and Teong, L K (2010). Recent trends, opportunities and challenges of biodiesel in Malaysia: An overview. *Renew. Sustain. Energy Rev.*, *14(3)*: 938-954.

Maleque, M A; Masjuki, H H and Haseeb, A S M A (2000). Effect of mechanical factors on tribological properties of palm oil methyl ester blended lubricant. *Wear*, *239(1)*: 117-125.

Mekhilef, S; Siga, S and Saidur, R (2011). A review on palm oil biodiesel as a source of renewable fuel. *Renew. Sustain. Energy Rev.*, *15(4)*: 1937-1949.

Mishra, V K and Goswami, R (2018). A review of production, properties and advantages of biodiesel. *Biofuels*, *9(2)*: 273-289.

Mohan, S; Dinesha, P and Bekal, S (2021). NO$_x$ reduction of biodiesel engine using pongamia ester with oleic acid and optimization of operating conditions using particle swarm optimization. *Int. J. Hydrog. Energy*, *46(52)*: 26665-26676.

Muhammed Niyas, M and Shaija, A (2022). Performance evaluation of diesel engine using biodiesels from waste coconut, sunflower, and palm cooking oils, and their hybrids. *Sustain. Energy Technol. Assess.*, *53*: 102681.

Mujtaba, M A; Muk Cho, H; Masjuki, H H; Kalam, M A; Farooq, M; Soudagar, M E M; Gul, M; Ahmed, W; Afzal, A; Bashir, S; Raju, V D; Yaqoob, H and Syahir, A Z (2021). Effect of alcoholic and nano-particles additives on tribological properties of diesel-palm-sesame-biodiesel blends. *Energy Rep.*, *7*: 1162-1171.

Öztürk, E and Can, Ö (2022). Effects of EGR, injection retardation and ethanol addition on combustion, performance and emissions of a DI diesel engine fueled with canola biodiesel/diesel fuel blend. *Energy*, 244: 123129.

Rahiman, M K; Santhoshkumar, S; Subramaniam, D; Avinash, A and Pugazhendhi, A (2022). Effects of oxygenated fuel pertaining to fuel analysis on diesel engine combustion and emission characteristics. *Energy*, 239: 122373.

Rajamohan, S; Gopal, A H; Muralidharan, K R; Huang, Z; Paramasivam, B; Ayyasamy, T; Nguyen, X P; Le, A T and Hoang, A T (2022). Evaluation of oxidation stability and engine behaviors operated by *Prosopis juliflora* biodiesel/diesel fuel blends with presence of synthetic antioxidant. *Sustain. Energy Technol. Assess.*, 52: 102086.

Rosha, P; Mohapatra, S K; Mahla, S K; Cho, H; Chauhan, B S and Dhir, A (2019). Effect of compression ratio on combustion, performance, and emission characteristics of compression ignition engine fueled with palm (B20) biodiesel blend. *Energy*, 178: 676-684.

Sakthivel, R; Ramesh, K; Purnachandran, R and Shameer, P M (2018). A review on the properties, performance and emission aspects of the third generation biodiesels. *Renew. Sustain. Energy Rev.*, 82: 2970-2992.

Sakthivel, R; Ramesh, K; Marshal, S J J and Sadasivuni, K K (2019). Prediction of performance and emission characteristics of diesel engine fuelled with waste biomass pyrolysis oil using response surface methodology. *Renew. Energy*, 136: 91-103.

Santhoshkumar, A; Thangarasu, V and Anand, R (2019). Chapter 12 - Performance, combustion, and emission characteristics of DI diesel engine using mahua biodiesel. *Advanced Biofuels*, (Azad, A K and Rasul, M eds.). Woodhead Publishing. p. 291-327.

Shahir, S A; Masjuki, H H; Kalam, M A; Imran, A and Ashraful, A M (2015). Performance and emission assessment of diesel-biodiesel-ethanol/bioethanol blend as a fuel in diesel engines: A review. *Renew. Sustain. Energy Rev.*, 48: 62-78.

Shote, A S; Betiku, E and Asere, A A (2019). Characteristics of CO and NO$_x$ emissions from combustion of transmethylated palm kernel oil-based biodiesel blends in a compression ignition engine. *J. King Saud Univ. - Eng. Sci.*, 31(2): 178-183.

Singh, Y; Singh, P; Sharma, A; Choudhary, P; Singla, A and Singh, N (2018). Optimization of wear and friction characteristics of *Phyllanthus emblica* seed oil based lubricant using response surface methodology. *Egypt. J. Pet.*, 27(4): 1145-1155.

Sorate, K A and Bhale, P V (2013). Impact of biodiesel on fuel system materials durability. *JSIR*, 72(01): 48-57.

Sorate, K A and Bhale, P V (2015). Biodiesel properties and automotive system compatibility issues. *Renew. Sustain. Energy Rev.*, 41: 777-798.

Sorate, K and Bhale, P (2018). Corrosion behavior of automotive materials with biodiesel: A different approach. *SAE Int. J. Fuels Lubr.*, 11(2): 147-162.

Tabatabaei, M; Aghbashlo, M; Dehhaghi, M; Kazemi Panahi, H S; Mollahosseini, A; Hosseini, M and Mojarab, M (2019). Reactor technologies for biodiesel production and processing: A review. *Prog. Energy Combust. Sci.*, 74: 239-303.

Tamilselvan, P; Nallusamy, N and Rajkumar, S (2017). A comprehensive review on performance, combustion and emission characteristics of biodiesel fuelled diesel engines. *Renew. Sustain. Energy Rev.*, 79: 1134-1159.

Tillis, P (2019). How the world got hooked on palm oil. *The Guardian*.

Verma, T N; Shrivastava, P; Rajak, U; Dwivedi, G; Jain, S; Zare, A; Shukla, A K and Verma, P (2021). A comprehensive review of the influence of physicochemical properties of biodiesel on combustion characteristics, engine performance and emissions. *J. Traffic Transp. Eng. Engl. Ed.*, 8(4): 510-533.

Yilmaz, N; Atmanli, A and Vigil, F M (2018). Quaternary blends of diesel, biodiesel, higher alcohols and vegetable oil in a compression ignition engine. *Fuel*, 212: 462-469.

Zaid, M; Kumar, A and Singh, Y (2021). Lubricity improvement of the raw jojoba oil with TiO$_2$ nanoparticles as an additives at different loads applied. *Mater. Today Proc.*, 46: 3165-3168.